Electrochemical oxidation of dibenzothiophene compounds on BDD electrode in acetonitrile–water medium

O. Ornelas Dávila[a], L. Lacalle Bergeron[b], P. Ruiz Gutiérrez[c], M.P. Elizalde González[c], M. M. Dávila Jiménez[a,*], I. Sirés[d], E. Brillas[d], A.F. Roig Navarro[b], J. Beltrán Arandes[b], J.V. Sancho Llopis[b]

[a] *Facultad de Ciencias Químicas, Benemérita Universidad Autónoma de Puebla, Mexico*

[b] *Instituto Universitario de Plaguicidas y Aguas (IUPA), Universidad Jaume I, Castellón de la Plana, Spain*

[c] *Centro de Química Instituto de Ciencias, Benemérita Universidad Autónoma de Puebla, Mexico*

[d] *Laboratori d'Electroquímica dels Materials i del Medi Ambient, Departament de Química Física, Facultat de Química, Universitat de Barcelona, Martí i Franquès 1-11, 08028 Barcelona, Spain*

* Corresponding author: E-mail address: mdavila.uap.mx@gmail.com

Tel.: +52-222-229-5525

Abstract

The electrochemical oxidation of dibenzothiophene and two derivatives, namely 4-methyldibenzothiophene and 4,6-dimethyldibenzothiophene, was investigated either separately or as a mixture, on a BDD anode in a miscible acetonitrile (87.5% v/v)–water (12.5% v/v, 0.01 M $NaNO_3$) solution. Linear sweep voltammetry, cyclic voltammetry, chronoamperometry and bulk electrolysis under potentiostatic conditions suggested the probable occurrence of two pathways: direct electrochemical oxidation and indirect reaction with hydroxyl radicals and other reactive oxygen species formed at the BDD anode surface during water discharge. The products extracted upon electrolysis at 1.5 and 2.0 V vs. SCE were analyzed by Fourier-transform infrared spectroscopy, gas chromatography–mass spectrometry and ultra-high performance liquid chromatography coupled to electrospray ionization and quadrupole time-of-flight mass spectrometry (UHPLC-ESI-Q-TOF-MS). The main molecules identified were the corresponding sulfoxides or sulfones, depending on the applied anodic potential. Possible oxidation routes for the dibenzothiophene compounds are proposed.

Keywords: BDD; Dibenzothiophenes; Electrochemical desulfurization; Sulfone; Sulfoxide

1. Introduction

The oxidation of alkyl sulfides is of considerable interest for practical applications, particularly in the hydrodesulfurization (HDS) of liquid fuels. Current HDS technologies are effective when applied to aliphatic and cyclic sulfur compounds but are less effective for the treatment of aromatic ones. These latter include dibenzothiophene (DBT) and derivatives such as 4-methyldibenzothiophene (4-MDBT) and 4,6-dimethyldibenzothiophene (4,6-DMDBT) (see molecular structures in Fig. 1), along with other derivatives present in diesel [1,2]. In recent years, oxidative desulfurization (ODS) has been recognized as a promising alternative process for sulfur removal [3-6], thus complementing current HDS technologies. Through the ODS process, refractory dibenzothiophene compounds and their alkylated derivatives present in liquid fuels can be converted into very polar sulfoxides or sulfones under mild conditions. Further, these products can be selectively extracted with various solvents [7,8].

A variety of oxidants may be used in the ODS process. Among these, H_2O_2 is attractive because it is commercially available and relatively cheap. This species can be combined in multiple ways: H_2O_2/acetic acid [9], H_2O_2/formic acid [10], and H_2O_2/heterogeneous catalyst [10,11]. Other reactive oxygen species (ROS) such as O_3, $O_2^{\bullet-}$ and $^{\bullet}OH$ can also oxidize the organic substances. These highly reactive species can be generated *in situ* by electrolysis of water present in the medium or upon the electrolyte decomposition [12–14]. In this context, electrochemical oxidation has been proposed as an effective alternative for removing sulfur, especially from diesel and gasoline.

Several articles have focused on electrochemical desulfurization (ECDS) as a new approach to liquid fuel desulfurization [15-20]. The ECDS method is advantageous compared to HDS since it is carried out at low reaction temperatures and pressures, in the absence of hydrogen. During the electrochemical oxidation under optimized working conditions, sulfur

aromatic compounds and their derivatives are easily oxidized to the corresponding sulfoxides and sulfones by direct electron transfer. These oxidized products can be subsequently removed by liquid-liquid extraction or adsorption techniques [21-24]. Simultaneously, ROS can also be produced from water electro-oxidation using anodes having different compositions, morphologies and structural properties [25-28]. ROS are then localized at an interface (e.g., electrode–solution, catalyst–solution). The most commonly employed electrodes to generate oxidizing species include vitreous carbon, PbO_2, dimensionally stable anodes (DSA®) and boron-doped diamond (BDD) [29]. The BDD electrode is the most efficient anode to mineralize contaminants like pesticides, dyes or drugs [30,31] contained in wastewater, which is due to its high oxidation power and large oxygen evolution overpotential. In some cases, however, it is not necessary to achieve total mineralization, but only to convert the parent molecule into more polar compounds that can be subsequently extracted from the medium. Oxidation studies on aromatic sulfur compounds have been carried out either in aprotic or aqueous media. However, less is known when mixtures of an aprotic medium and water are employed and, more important, which is the contribution of water in the reaction route. To gain deeper knowledge on the role of water in the ODS of dibenzothiophenes when mixed with acetonitrile, an exhaustive study dealing with the electrochemical reactivity of DBT, 4-MDBT and 4,6-DMDBT has been undertaken for the first time. This has allowed clarifying the reaction mechanisms to yield their respective sulfoxides or sulfones under mild electrolysis conditions using a BDD anode. Electroanalytical techniques like linear sweep voltammetry, cyclic voltammetry, chronoamperometry and bulk electrolysis, as well as analytical methods like FTIR, UV/Vis, UHPLC-ESI-Q-TOF-MS and GC-MS, have been utilized. The contributions of direct and mediated oxidation during the electro-oxidation process of benzothiphenes were examined and reliable oxidation pathways for each compound were elucidated.

2. Materials and methods

2.1. Reagents and preparation of solutions

DBT (99% purity), 4-MDBT (96% purity), 4,6-DMDBT (97% purity), methanol and hexane of chromatographic grade, and $NaNO_3$ were purchased from Sigma Aldrich. Acetonitrile ACS/HPLC provided by Burdick & Jackson and ultrapure water (18.2 MΩ ·cm) from a Milli-Q system were used to prepare the acetonitrile/water solutions. For the electrochemical studies, single solutions were prepared by dissolving DBT, 4-MDBT or 4,6-DMDBT, separately, first in acetonitrile for 30–45 min with mechanical stirring. Then, the appropriate volumes of 0.01 M $NaNO_3$ aqueous solution were added to obtain an acetonitrile (87.5% v/v)–water (12.5% v/v, 0.01 M $NaNO_3$) mixture. DBT + 4-MDBT + 4,6-DMDBT mixtures in the above medium were also prepared to clarify the electrochemical reactivities.

2.2. Electrochemical analysis

DBT and its alkylated derivatives 4-MDBT and 4,6-DMDBT are poorly soluble in water and confer low conductivity. Therefore, acetonitrile was employed as a co-solvent and $NaNO_3$ as the electrolyte. The acetonitrile (87.5% v/v)–water (12.5% v/v, 0.01 M $NaNO_3$) mixture was suitable for investigating the electrochemical oxidation and bulk electrolysis of all dibenzothiophenes. First, the BDD electrode was cycled (over 5 cycles) from –2.00 to 2.00 V vs. SCE at 10 mV s^{-1} in a given solution. The electrochemical measurements and bulk electrolyses of the dibenzothiophenic compounds were carried out in an undivided cell of 80 mL comprising three electrodes and the acetonitrile (87.5% v/v)–water (12.5% v/v, 0.01 M $NaNO_3$) medium. The anode and counter electrode were commercial boron-doped diamond (BDD) thin films deposited onto niobium mesh substrates, purchased from Condias (Germany), with a geometrical area of 20 cm^2 each. SCE (3 M KCl) was employed as the reference electrode, and all potentials are referred to it. The electrochemical measurements

were carried out using an Autolab PGSTAT 302 potentiostat/galvanostat from Eco Chemie, controlled by GPES 4.9 software. The electrochemical response and stability of the BDD anode was tested by recording cyclic voltammograms before and after each experiment.

2.3. Equipment and analysis conditions

2.3.1. GC-MS analysis

After evaporating the electrolyzed solutions, the solid phase was dissolved in methanol and hexane to analyze the oxidized products using gas chromatography (GC) equipped with an ion-trap mass spectrometer (MS). A Varian CP-3800 gas chromatograph coupled to a mass spectrometry detector (Saturn 4000, Varian) was used to identify the molecules, which were separated on a Supelcowax 10 (30 m × 0.25 mm, 0.25 μm film thickness) capillary column, using helium as carrier gas at a constant flowrate of 1 mL min^{-1}. The temperature program was: 70 °C for 2 min, increase to 150 °C at 30 °C min^{-1} and then, increase to 250 °C at 5 °C min^{-1}, with a final isothermal stage of 25.33 min. Injection of 1 μL of sample in splitless mode (injection port temperature of 220 °C) was performed using a Varian 8400 autosampler equipped with a 10 μL syringe. Ion trap MS determinations were carried out in full scan mode (*m/z* scan range of 40 – 600 Da) using electron impact ionization (70 eV) in positive mode and external ionization configuration. GC-MS interface; ion trap and manifold temperatures were set at 275 °C, 190 °C and 60 °C, respectively.

2.3.2. UHPLC-ESI-Q-TOF-MS analysis

The electrolyzed solutions were concentrated by evaporation. Then, they were diluted (1:100) for the analysis of the products by UHPLC-ESI-Q-TOF-MS. The modern Q-TOF-MS instruments allow the simultaneous acquisition of two full spectra acquisition functions with different collision energies in a single injection (MSE mode). Using the low energy function (LE) with a collision energy of 4 eV, the information obtained corresponds normally

to non-fragmented ions, related to the parent protonated molecule $[M+H]^+$ in positive ionization mode. The high energy function (HE), with a collision energy ramp ranging from 15 to 40 eV, is selected in order to obtain a wide range of fragmented ions.

The analysis was carried out with a Waters Acquity ultra-performance liquid chromatography (UPLC) system (Waters, Milford). The chromatographic separation was performed using an Acquity UPLC BEH C18 (2.1 mm × 100 mm, 1.7 µm particle size) analytical column from Waters. The mobile phases used were A (water) and B (methanol), both with 0.01% formic acid. The percentage of B changed as follows: 0 min, 10%; 14 min, 90%; and 16.10 min, 10%. The flowrate was 300 $\mu L \cdot min^{-1}$ and the analysis run time was 18 min. The sample injection volume was 20 µL. The UPLC system was interfaced to a hybrid quadrupole-TOF high resolution (HRMS) mass spectrometer (Xevo G2 Q-TOF, Waters Micromass), using an orthogonal Z-spray-ESI interface operating in both positive and negative ion mode. TOF-MS resolution was approximately 25000 at full width half maximum at *m/z* 556. Nitrogen was used as drying gas and nebulizing gas. The gas flow was set at 800 $L \cdot h^{-1}$. MS data were acquired over an *m/z* range of 50-1200 at a scan time of 0.4 s. A capillary voltage of 0.7 kV and cone voltage of 20 V were used in positive ionization mode. Collision gas was argon 99.995% (Praxair). The interface, source and column temperatures were set at 450 ºC, 150 ºC, and 40 ºC, respectively.

2.3.3. ICP-MS analysis

Qualitative determination of niobium in electrolyzed solutions was conducted with an Agilent 7500cx ICP-MS instrument. For that purpose, the selected samples were evaporated to dryness and redissolved with 2 mL of 1% HNO_3. Afterwards, samples were nebulized to the ICP-MS and *m/z* 93 was monitored in qualitative mode (20 points per peak). Reagents free of Nb were checked from the analysis of blank solutions (1% HNO_3).

156 *2.3.4. UV/Vis analysis and FTIR spectroscopy*

157 Hydrogen peroxide formed during the electrolysis in the reaction medium was analyzed
158 using UV/Vis spectrophotometry (HACH DR 5000) over the range 200–800 nm. The IR
159 spectra were recorded over the range 400–4000 cm^{-1} using a Nicolet 6700 spectrometer from
160 Thermo Scientific and pressed KBr pellets.

161 **3. Results and discussion**

162 *3.1. Electrochemical response of the BDD electrode in acetonitrile–water medium*

163 Linear sweep and cyclic voltammograms were recorded in water and in acetonitrile–
164 water mixtures containing 0.01 M $NaNO_3$ as the electrolyte. Different acetonitrile and water
165 proportions were used and DBT was added to test the electrochemical response of the BDD
166 working electrode and the discharge of water and solvent. The linear sweep voltammograms
167 obtained in the different electrolytic media are shown in Fig. 2. These curves were recorded
168 from -0.50 V, although they are presented starting from 0.50 V to better observe the oxidation
169 process. The use of 12.5% water with 0.01 M $NaNO_3$ yielded a greater anodic current due to
170 the decomposition of water present in the reaction medium (Fig. 2, curve (a)). The anodic
171 current increased considerably in the presence of a much larger amount of water, i.e., 87.5%
172 (Fig. 2, curve (b)). In acetonitrile (12.5%)–water (87.5%, 0.01 M $NaNO_3$) or in 100% water
173 with 0.01 M $NaNO_3$ (Fig. 2, curve (c)), the onset potential for water discharge was less anodic
174 (see inset of Fig. 2). In these cases, the anodic current was high in the potential range 1.50-
175 2.00 V (Fig. 2, curves (b) and (c)). The onset potentials were of 1.655, 1.386 and 1.524 V in
176 acetonitrile (87.5%)–water (12.5%), acetonitrile (12.5%)–water (87.5%) and 100% water,
177 respectively.

178 On the other hand, oxygen evolution from water oxidation on a BDD electrode requires
179 a large overpotential and the mechanism involves the formation of $^{\bullet}OH$ as intermediate in

the oxygen evolution reaction. According to some authors [13,32], a decrease in the oxygen evolution rate occurs in the presence of aprotic and protic solvents due to competition with $^{\bullet}OH$. The latter may be responsible for the low current observed within the potential interval from 1.50 to 2.00 V in the presence of an excess of acetonitrile.

3.2. Linear polarization curves for the electrochemical oxidation of DBT, 4-MDBT and 4,6-DMDBT

The electrochemical behavior of DBT, 4-MDBT, and 4,6-DMDBT on BDD was studied separately by means of linear sweep voltammetry. Fig. 3a shows the profiles obtained in the absence of dibenzothiophenes as well as in the presence of 67 mg L^{-1} DBT (curve (a)), 86 mg L^{-1} 4-MDBT (curve (b)) and 86 mg L^{-1} 4,6-DMBDT (curve (c)). These concentrations were selected so as to ensure the good resolution of peaks. These curves revealed no obvious oxidation peaks, although subtraction of the background electrolyte current in Fig. 3b shows a maximum current near the onset decomposition potential of water for DBT (curve (a')), 4-MDBT (curve (b')) and 4,6-DMDBT (curve (c')). The potentials at which the maximum anodic currents appeared were 1.96, 1.90 and 1.91 V for such compounds, respectively. This means that the three dibenzothiophenes are directly oxidized at the BDD surface before water discharge, although their removal is enhanced when the latter process occurs since it yields the strong oxidant $^{\bullet}OH$, which promotes the mediated oxidation. These peaks can be attributed to the formation of sulfone groups ($DBTO_2$) via oxidation of the corresponding dibenzothiophene sulfoxide (DBTO), as demonstrated below. Note that the formation of $DBTO_2$ around 2.00 V on a glassy carbon electrode in acetonitrile medium and in the presence of water has been previously reported [33].

The above linear voltammograms also revealed that, at potential values exceeding the onset value of 1.165 V, the anodic currents increased markedly. This trend was attributed to the direct electro-oxidation of the dibenzothiophene compounds and, at potentials higher than

205 1.9 V, to the decomposition of water present in the reaction medium, which generated
206 reactive oxidants such as •OH, O_3, H_2O_2 and O_2 [25,29]. On the other hand, the onset
207 oxidation potentials for 67 mg L^{-1} DBT and 86 mg L^{-1} 4-MDBT were very similar and
208 slightly higher than 1.224 V (curves (a') and (b') in Fig. 3b). The 86 mg L^{-1} 4,6-DMDBT
209 profile revealed a much lower onset oxidation potential of 0.790 V (curve (c')). In addition,
210 a small oxidation peak appeared around 1.038 V (Fig. 3a and b, curves (c) and (c')) within
211 the region of the water stability (Fig. 2). The anodic peak that appeared at 1.038–1.150 V
212 within the low potential region, as well as the low maximum anodic current observed in Fig.
213 3b, curve (c'), suggests the electrochemical oxidation of 4,6-DMDBT by an electrochemical–
214 chemical oxidation mechanism similar those proposed for DBT [33,34], diaryl sulfides [35]
215 and aliphatic sulfides [36]. It means that the direct electrochemical oxidation of 4,6-DMDBT
216 occurred in the potential region corresponding to water stability. This was corroborated upon
217 bulk electrolysis of 4,6-DMDBT (86 mg L^{-1}) at 1.15 V over a long period of time of 16 h.
218 The main product identified in the electrolyzed extract by UHPLC-ESI-Q-TOF-MS was 4,6-
219 dimethyldibenzothiophene sulfoxide (4,6-DMDBTO).

220 We aimed to study the electrochemical reactivity of DBT and 4,6-DMDBT by
221 comparing the linear sweep voltammograms at a lower concentration of 20 mg L^{-1} DBT and
222 4,6-DMDBT at 20 mV s^{-1}, after subtracting the background electrolyte current (data not
223 shown). These results showed that the first oxidation step occurred at 1649 mV for DBT and
224 at 1580 mV for 4,6-DMDBT. On the other hand, the smaller anodic peak at 1.038–1.150 V
225 suggested that 4,6-DMDBT was more electrochemically reactive than DBT. The reactivity
226 of alkyl dibenzothiophenes in desulfurization processes could be described using theoretical
227 descriptors like the local, global and molecular electrostatic potential [37]. The oxidation
228 reactivity of sulfur compounds is reported to increase with the electron density on the sulfur
229 atom [7]. In this context, the higher electron densities (5.760) of the sulfur atoms in 4,6-

DMDBT and 4-MDBT (5.759) rendered more favorable the anodic oxidation as compared to DBT (5.758). These results agree with the reactivity of DBT and alkyl dibenzothiophenes reported during oxidative desulfurization of light gas oil [7] and fuel oils using the ODS methods [10,11].

3.3. Cyclic voltammetry with DBT, 4-MDBT and 4,6-DMDBT solutions

The cyclic voltammograms for the oxidation of 67 mg L^{-1} DBT and 86 mg L^{-1} 4-MDBT and 4,6-DMDBT revealed that their oxidation on BDD surface occurred around 1.20 V, showing the highest anodic currents between 1.50 and 2.00 V (Fig. 4a, curves (a)–(c)). Worth commenting, all voltammograms were initiated at -2.00 V, near the cathodic discharge of water to hydrogen and OH^-, although the profiles presented in Fig. 4 start at -0.50 V to better observe the anodic oxidation. No reduction peaks were found during the cathodic scans down to -2.00 V, meaning that the oxidation process was irreversible, probably due to the fast reactions of cation radicals (after abstracting one electron from sulfur) with water molecules present in the reaction medium [33-36].

The effect of electrode fouling was tested by recording consecutive cyclic voltammograms during the anodic oxidation of 200 mg L^{-1} DBT and 4,6-DMDBT at a scan rate of 10 mV s^{-1}. The changes in current during the first five cycles overlapped for 200 mg L^{-1} DBT (Fig. 4b, curve (a)) and 4,6-DMDBT (Fig. 4b, curve (b)). The current at anodic potential (E_{an}) = 2.00 V decreased by 9% after 44 cycles for 200 mg L^{-1} 4,6-DMDBT (Fig. 4b, curve (b)). This behavior and the fact that no specific peaks were found in the voltammograms, indicates that the oxidation products resulting from the parent compounds did not adsorb onto BDD. On the other hand, the cyclic voltammograms revealed that the anodic current in the presence of the sulfur compounds increased at potentials greater than 1.50 V, indicating their oxidation. For this reason, the anodic oxidations of DBT and 4,6-DMDBT were investigated by electrolysis at constant potential. The extracts obtained after

bulk electrolysis of these molecules for 4 h at 1.50 V in acetonitrile (87.5% v/v)–water (12.5% v/v, 0.01 M $NaNO_3$) were analyzed by GC-MS and UHPLC-ESI-Q-TOF-MS, confirming that DBTO and 4,6-dimethydibenzothiophene sulfoxide (4,6-DMDBO) were formed at this potential pre-eminently via direct electrochemical oxidation. Bulk electrolysis at 2.00 V for 4 h yielded dibenzothiophene sulfone ($DBTO_2$) and 4,6-dimethyldibenzothiophene sulfone (4,6-$DMDBTO_2$) as the main products.

The anodic current depended on the concentration of the dibenzothiophene compounds present in the reaction medium. The potentiodynamic curves shown in Fig. 5a and b revealed that 30 mg L^{-1} DBT (curve (a)) or 4, 6-DMDBT (curve (a')) presented one oxidation wave around 1.74 and 1.61 V, respectively. This figure also depicts that the onset for DBT oxidation was shifted to lower positive values at higher concentrations of the compound. The shifts of the *I-E* curves toward lower potentials indicated that DBT and 4,6-DMDBT oxidation also occurred through hydroxyl radicals. However, the anodic current was low in the interval potentials from 1.00 to 1.35 V, but increased dramatically at $E_{an} > 1.35$ V. This behavior of the oxidation current as a function of the potential and concentration evidences that DBT and 4,6-DMDBT oxidation processes were accompanied by other oxidation reactions that occurred simultaneously. Fig. 5a and b also indicate that the anodic current depended strongly on the sulfur compound concentration, reaching potentials exceeding 1.75 V, where water decomposition occurred. For this reason, at $E_{an} > 1.75$ V, the indirect oxidation of sulfur compounds can be assumed, mediated by electrogenerated $^{\bullet}OH$ (and other ROS), along with direct electron transfer at the BDD anode surface. The water oxidation then contributed to the total anodic current. The shift of the onset values for of DBT and 4,6-DMDBT oxidation and the dependence of the maximum anodic current on concentration were more evident when the background current was subtracted upon linear polarization (Fig. 6a and b). These curves revealed a linear dependence of the anodic current on the

concentration of compounds over a potential range between 1.25 and 1.90 V (insets in Fig. 6a and b). A linear dependence was also obtained when plotting I_p vs. $v^{½}$ during the voltammetric studies, as expected if the oxidation of both, DBT and 4,6-DMDBT, was controlled by mass transport.

At high concentrations, the start of the anodic oxidation was more pronounced (insets showing *E* vs. concentration at a constant current). The low current in the potential region from 0.80 to 1.35 V for the dibenzothiophene compounds indicate that the direct oxidation process occurred and did not play a prominent role in the overall electrochemical oxidation. This is in agreement with the quasi-polarization curves of log *I* vs. *E*, as shown in Fig. 5 (insets) for the electro-oxidation of DBT and 4,6-DMDBT at the BDD anode, where two Tafel slopes can be observed. The Tafel slopes for DBT in the low potential range varied from 262 to 271 mV dec^{-1}, and the reaction order with respect to DBT was 0.62. In the case of 4,6-DMDBT, the Tafel slopes within the low potential range varied from 238 to 333 mV dec^{-1} and the reaction order was 0.51. The high values of the Tafel slopes and the low reaction order possibly arose either from the BDD film deposit onto the porous Nb substrate [38,39] or from a first slow charge transfer step. These values also indicate that the oxidation of these compounds occurred through a multi-stage mechanism, as described previously [33-36]. The feasible mechanism (direct or indirect oxidation) operating at $E_{an} < 1.50$ V or $1.70 \leq E_{an} \leq 2.00$ V was explored using chronoamperometric measurements.

3.4. Chronoamperometric study

In an anhydrous aprotic solvent, it is easy to discern whether the oxidation of an organic compound occurs via direct oxidation; however, the electrochemical oxidation of the dibenzothiophenic compounds in acetonitrile–water was very difficult to characterize in terms of direct electron transfer or mediated oxidation mechanisms. Chronoamperometric experiments were carried out to study the electrochemical oxidation of DBT or 4,6-DMDBT

within the potential interval 1.15–2.00 V. Fig. 7 presents the potentiostatic *I–t* curves obtained for different 4,6-DMDBT concentrations at several applied potentials using quiescent solutions. As shown in these curves, the anodic current depended on the concentration of 4,6-DMDBT. The current difference between the electrolyte solution prepared with or without 4,6-DMDBT supported the direct transfer of electrons at the anode surface. Higher current reaction steps (i.e., the space between the current in the presence and absence of 4,6-DMDBT) indicated better direct electrochemical oxidation of the compound at the electrode surface. A low applied potential (1.150 V) produced no appreciable changes in the anodic currents of the 4,6-DMDBT solution or the electrolyte (Fig. 7a). These results allowed inferring that direct oxidation was not efficient, but, if the potential rose from 1.50 to 2.00 V, the anodic current increased significantly. At $E_{an} \geq 1.50$ V, significant differences were observed between the steady state currents of the solution containing 4,6-DMDBT (Fig. 7b and c) and the supporting electrolyte. This evidences that oxidation occurred more favorably through direct electron transfer in this potential region. On the other hand, the *I* vs. concentration plots obtained at the three different potentials displayed a good linear dependence over the range 30–200 mg L^{-1} (insets in Fig. 7), confirming the electrochemical decomposition of water and simultaneous direct electrochemical oxidation of 4,6-DMDBT. As previously reported [12,25], an acidic aqueous medium promotes the formation of hydroxyl radical and H_2O_2 at the BDD electrode as a result of water discharge according to the following reactions:

$$BDD + H_2O \rightarrow BDD(^{\bullet}OH) + H^+ + e^- \quad (1)$$

$$2BDD(^{\bullet}OH) \rightarrow 2BDD + H_2O_2 \quad (2)$$

$$2BDD(^{\bullet}OH) \rightarrow 2BDD + O_2 + 2H^+ + 2e^- \quad (3)$$

In our case, the hydroxyl radical formed through direct electro-oxidation of water at the electrode surface (reaction (1)) facilitated the formation of H_2O_2 near the electrode surface via reaction (2). The production of hydroxyl radical on the anode BDD surface was assessed by chronoamperometry measuring the current upon the step-by-step injection of water into the solution under polarization of the BDD anode at 1.75 or 2.00 V. As can be seen in Fig. 8a, the water addition to the reaction medium in the absence of 4,6-DMDBT caused a current increase (inset in Fig.8a). This finding agrees with the formation of hydroxyl radical on the anode surface via direct electron transfer according to reaction (1). At the same potential, in the presence of 4,6-DMDBT (Fig. 8b), a steady-state current was enhanced when its concentration was increased, as show in inset in Fig. 8b. This indicates that, at this potential, direct electron transfer occurred during 4,6-DMDBT oxidation in parallel with water discharge. Direct electron transfer in parallel to the indirect reaction of hydroxyl radicals has been reported for several organic pollutants [40,41]. Nevertheless, at E_{an} > 1.75 V, the electrogenerated hydroxyl radicals may self-react to form H_2O_2 by reaction (2) or evolve to O_2 gas via reaction (3) [25].

The production of H_2O_2 during the main electrolysis reaction in acetonitrile (87.5%)–water (12.5%, 0.01 M $NaNO_3$) at 2.00 V was demonstrated using a spectrophotometric method based on the well-known formation of the Ti(IV)-H_2O_2 complex, as exemplified in SM Fig. S1.

3.5. Electrolyses under potentiostatic conditions

Bulk electrolysis assays for DBT, 4-MDBT and 4,6-DMDBT were carried out either with single compounds or with a mixture, at 1.50 and 2.00 V, for 4 h. During these trials, the anodic current at 2.00 V was higher than that at 1.50 V due to water oxidation. No passivation of the BDD anode, as a result of possible fouling by polymerization of the target organic

352 sulfur compounds or their by-products, was observed, as also described in the voltammetric
353 study of section 3.3. Electrolysis at 2.00 V caused direct electro-oxidation and, in parallel,
354 indirect reaction. A potential of E_{an} < 1.75 V induced sulfur compound oxidation, as
355 described above, through direct multi-stage electron transfer [33-36]. To better understand
356 these points, analysis of the extracted products after bulk electrolysis was carried out by
357 FTIR, GC-MS and UPLC-MS.

358 *3.5.1. IR spectroscopic analysis of the extracted products*

359 SM Fig. S2a-c depict the IR spectra of extracts of the dibenzothiophene compounds
360 before and after oxidation. The infrared spectra obtained after electrochemical oxidation at
361 1.50 or 2.00 V revealed absorption bands corresponding to S-O vibrations in the range 600–
362 500 cm^{-1}. The C-S stretching frequencies between 700 and 800 cm^{-1} shifted after oxidation
363 of 4-MDBT (Fig. S2a) and 4,6-DMDBT (Fig. S2b). The IR spectra of samples treated at 1.50
364 and 2.00 V were compared with the spectra obtained from DBT-sulfone (Fig. S2c). All
365 standard DBT-sulfone vibrations were present in the extracts of the treated samples. The
366 sulfoxide and sulfone compounds formed were confirmed using GC-MS and UHPLC-ESI-
367 Q-TOF-MS.

368 *3.5.2. GC-MS analysis*

369 After oxidation of the dibenzothiophene compounds at 1.50 and 2.00 V, the extracts were
370 analyzed by GC-MS. SM Fig. S3a and S3b display the chromatograms and MS spectra
371 corresponding to electrolysis of 4,6-DMDBT, whereas SM Fig. S4a and S4b show those of
372 DBT. The peaks observed in the chromatograms obtained at retention time (t_r) = 37.94 min
373 (Fig. S4b, (b)) and t_r = 35.10 min (Fig. S3b, (b)), along with the MS spectra obtained at *m/z*
374 = 216 (Fig. S4b) and *m/z* = 244 (Fig. S3b), corresponded to the molecular ion peaks of $DBTO_2$
375 and 4,6-$DMDBTO_2$, respectively, according with NIST database (match 84%). Analysis of

376 the chromatograms shown in Fig. S3a and S4a revealed that the formation of 4,6-DMDBTO_2
377 was favored at 2.00 V, with the removal of 99.2% 4,6-DMDBT after 4 h of electrolysis. The
378 removal of 97.5% DBT at the same potential required a greater electrolysis time of 6 h. These
379 results suggests that 4,6-DMDBT was more prone to undergo anodic oxidation.
380 Bulk electrolysis of a model mixture containing DBT + 4-MDBT + 4,6-DMDBT was
381 conducted over 4 h at 1.50 and 2.00 V with the aim of assessing the reactivity of each
382 compound and possible interference (or interaction) between the three compounds. SM Fig.
383 S5a and S5b show chromatograms and mass spectra obtained from solutions extracted with
384 methanol after bulk electrolysis of a solution of dibenzothiophene compounds. An inspection
385 of the chromatograms reveals that the peak areas of DBT, 4-MDBT and 4,6-DMDBT
386 decreased markedly after bulk electrolysis at 2.00 was compared to 1.50 V, and the formation
387 of the P1, P2, and P3 products were more favored at 2.00 V (Fig. S5a-(c)). These
388 chromatograms evidence that the dibenzothiophene compounds were not completely
389 oxidized at 1.50 V (Fig. S5a-(b)) or at 2.00 V (Fig. S5a-(c)) after 4 h of electrolysis. Few
390 compounds remained in the mixture after electrolysis, since 99.4% DBT, 97.7% 4-MDBT
391 and 99.7% 4,6-DMDBT were removed from the mixture. The mass spectra (Fig. S5b)
392 highlight that the reaction products arising from the dibenzothiophene compounds in the
393 mixture after electrolysis were DBTO_2, 4-MDBTO_2 and 4,6-DMDBTO_2. They were
394 identified by comparing the retention times of pure compounds with NIST database. As
395 shown in the chromatogram (c) of Fig. S5a, the simultaneous electrochemical oxidation of a
396 mixture at 2.00 V preferably oxidized 4,6-DMDBT to its corresponding 4,6-DMDBTO_2 (t_r
397 = 35.07 min), as inferred from the intensity and area of the peak. These findings indicate that
398 the sulfur compounds contained in the mixture were pre-eminently oxidized in the order: 4,6-
399 DMDBT ≥ 4-MDBT > DBT. This agrees with the oxidation results obtained from ODS

400 studies using different catalyst/hydroxide peroxide systems [11,17]. The oxidation products
401 described above were confirmed using UHPLC-ESI-Q-TOF-MS analysis.

402 *3.5.3. UHPLC-ESI-Q-TOF-MS analysis*

403 The results obtained through UHPLC-ESI-Q-TOF-MS analysis of the extracts of DBT,
404 4-MDBT and 4,6-DMDBT at different potentials revealed that the electrochemical oxidation
405 process at the BDD electrode in acetonitrile (87.5%)–water (12.5%, 0.01 M $NaNO_3$) was a
406 selective oxidation reaction. The total ion chromatograms of the oxidation products of 4-
407 MDBT and 4,6-DMDBT after bulk electrolysis of each single compound at 2.00 V displayed
408 only one peak at t_r of 7.24 and 8.43 min, respectively. Their mass spectra at low and high
409 energy confirmed that the most important anodic oxidation products corresponded to 4-
410 $MDBTO_2$ and 4,6-$DMDBTO_2$, respectively. No other peaks were observed, meaning that
411 there is no intermediate formation or degradation of the molecules under the analysis
412 conditions. In the case of the simultaneous electrochemical oxidation of a mixture DBT + 4-
413 MDBT + 4,6-DMDBT at 1.50 V, 4,6-DMDBT was preferably oxidized to 4,6-DMDBT
414 sulfoxide (SM Fig. S6a). It can be seen in the chromatogram of Fig. S6b that the oxidation
415 of the mixture at 2.00 V yielded the corresponding sulfones of DBT and 4-MDBT in a minor
416 proportion. These results indicate that the 4,6-DMDBT oxidation is favored at 1.50 and 2.00
417 V and that the effect of the anodic potential is evident in the conversion of the sulfur
418 compounds to their corresponding sulfoxides or sulfones. The mass spectra at low collision
419 energy (LE) and high collision energy (HE) of the corresponding sulfoxides and sulfones are
420 shown in the SM Fig. S7-S9. The 4,6-DMDBT oxidation was favored at E_{an} > 1.50 V and
421 E_{an} = 2.00 V when it was present either alone or in the mixture. These findings suggest that
422 under the applied potentials, the dibenzothiophene compounds were selectively oxidized by
423 direct and indirect pathways to their corresponding sulfoxides and sulfones without breaking

or mineralizing the aromatic sulfur compounds. The oxidation pathways can then be described as proposed in Fig. 9 and 10.

During the electrolysis of a DBT + 4-MDBT + 4,6-DMBDT mixture in the presence of water at 2.0 V, an excess of ROS is formed. According to the results of the analysis for the electrolyzed solutions by GC-MS and UHPLC-ESI-Q-TOF-MS, these compounds did not compete between them to react with generated ROS. At E_{an} = 1.50 V, the ratio of these species relative to the substrate in the mixture was low, and only partial conversion was achieved, as described in Fig. 10.

One of the ROS formed during the discharge of water is H_2O_2 and then, this oxidizing compound is expected to contribute to the indirect oxidation reaction of the aromatic sulfur compounds. At E_{an} > 1.75 V, the dibenzothiophene compounds were directly oxidized on the BDD electrode. Simultaneously, H_2O_2 was generated *in situ* from reactions (1) and (2) and reacted with the sulfur compounds according to the mechanism proposed in Fig. 11, as also reported previously [42].

3.6. Mechanism underlying the direct anodic oxidation of dibenzothiophene compounds on the BDD electrode

Previous publications have pointed out that the oxidation of organic sulfur compounds depends on the water content in acetonitrile [33,36]. Fig. 12 shows a mechanism proposed for the direct anodic oxidation of dibenzothiophenes. It is initiated by an electrochemical step in which an electron is taken from the sulfur atom to yield the reacting cation residue $[DBT]^{\bullet+}$. This cation rapidly undergoes proton loss to yield sulfoxide and other intermediates, followed by a second electron loss to form the sulfone.

3.7. BBD electrode stability

The BDD electrode tends to undergo fouling and it is susceptible to delamination or corrosion in the presence of organic compounds at high potentials [43]. The BDD film

surface can also undergo morphological changes. In this context, the BDD anode surface was analyzed by scanning electron microscopy (SEM) after prolonged electrolysis times of 16 h at 2.00 and 3.00 V and after prolonged repetitive cycling of 14 h over a potential interval of –0.50 to 2.00 V at 10 mV s^{-1}, in the absence and in the presence of 4,6-DMDBT. This analysis was carried out with a JEOL JSM-7800F and revealed that the BDD surface did not undergo neither fouling nor evident morphological changes, as exemplified in SM Fig. S10. The possibility of anodic dissolution of the niobium support in acetonitrile–water after the above assays was also analyzed using ICP-MS. A niobium concentration exceeding 5 ppb was detected. Since this metal is anodically resistive, the detected niobium ions with *m/z* 93 must have been produced by electrochemical corrosion of the NbC layer formed during the deposition of the BDD film [44].

4. Conclusions

The selective electrochemical oxidation of DBT, 4-MDBT and 4,6-DMDBT to their corresponding sulfoxides or sulfones on BDD anode depended on the applied potential during bulk electrolysis, the water content in the reaction medium and the concentrations of the sulfur compounds. The electrochemical oxidation of a mixture of sulfur compounds containing DBT + 4-MDBT + 4,6-DMDBT revealed that, in acetonitrile (87.5%) –water (12.5%, 0.01 M $NaNO_3$), the reactivity decreased in the order 4,6-DMDBT ≥ 4-MDBT > DBT. The electrochemical oxidation of these compounds occurred at E_{an} ≥ 1.75 V, simultaneously by direct electron transfer at the BDD surface and through ROS that were generated during the electrolysis of water present in the reaction medium. This anodic process was characterized using electrochemical techniques and the corresponding sulfoxides or sulfones were detected by several analytical techniques. Oxidation routes are proposed to explain the formation of such products from each dibenzothiophene compound.

Acknowledgments

This work was funded by the Benemérita Universidad Autónoma de Puebla (VIEP-BUAP) and by SEP-DGESU. O. Ornelas is grateful for the postdoctoral grant (PRODEP) No. DSA/103.5/16/14302. Support from R. Silva (IFUAP) for SEM analysis is also acknowledged.

References

[1] C. Song, An overview of new approaches to deep desulfurization for ultra-clean gasoline, diesel fuel and jet fuel, Catal. Today 86 (2003) 211-263.

[2] S.K. Bej, S.K. Maity, U.T. Turaga, Search for an efficient 4,6-DMDBT hydrodesulfurization catalyst. A review of recent studies, Energy Fuels 18 (2004) 1227-1237.

[3] J.L. García-Gutiérrez, I.P. Lozano, F. Hernández-Pérez, G.C. Laredo, F. Jimenez-Cruz, R & D in oxidative desulfurization of fuels technologies: from chemistry to patents, Recent Pat. Chem. Eng. 5 (2012) 174-196.

[4] F.S. Mjalli, O.U. Ahmed, T. Al-Wahaibi, Y. Al-Wahaibi, I.M. Al Nashef, Deep oxidative desulfurization of liquid fuels, Rev. Chem. Eng. 30 (2014) 337-378.

[5] S.-Y. Dou, R. Wang, Recent advances in new catalysts for fuel oil desulfurization, Curr. Org. Chem. 21 (2017) 1019-1036.

[6] M.N. Hossain H.C. Park, H.S. Choi, A comprehensive review on catalytic oxidative desulfurization of liquid fuel oil, Catalysts 9 (2019) 229 (12 pages).

[7] D. Zheng, W. Zhu, S. Xun, M. Zhou, M. Zhang, W. Jiang, Y. Qin, H. Li, Deep oxidative desulfurization of dibenzothiophene using low-temperature-mediated titanium dioxide catalyst in ionic liquids, Fuel 159 (2015) 446-453.

[8] Y. Li, Y. Zhang, P. Wu, C. Feng, G. Xue, Catalytic oxidative/extractive desulfurization of model oil using transition metal substituted phosphomolybdates-based ionic liquids, Catalysts 8 (2018) 639 (13 pages).

[9] A. Haghighat Mamaghani, S. Fatemi, M. Asgari, Investigation of influential parameters in deep oxidative desulfurization of dibenzothiophene with hydrogen peroxide and formic acid, Int. J. Chem. Eng. 2013 (2013) 1-10.

[10] M. Te, C. Fairbridge, Z. Ring, Oxidation reactivities of dibenzothiophenes in polyoxometalate/H_2O_2 and formic acid/H_2O_2 systems, Appl. Catal. A: Gen. 219 (2001) 267-280.

[11] F. Al-Shahrani, T. Xiao, S.A. Llewellyn, S. Barri, Z. Jiang, H. Shi, G. Martinie, M.L.H. Green, Desulfurization of diesel via the H_2O_2 oxidation of aromatic sulfides to sulfones using a tungstate catalyst, Appl. Catal. B: Environ. 73 (2007) 311-316.

[12] P.A. Michaud, M. Panizza, L. Ouattara, T. Diaco, G. Foti, Ch. Comninellis, Electrochemical oxidation of water on synthetic boron-doped diamond thin film anodes, J. Appl. Electrochem. 33 (2003) 151-154.

[13] I. Kisacik, A. Stefanova, S. Ernst, H. Baltruschat, Oxidation of carbon monoxide, hydrogen peroxide and water at a boron doped diamond electrode: the competition for hydroxyl radicals, Phys. Chem. Chem. Phys. 15 (2013) 4616-4624.

[14] B. Marselli, J. García-Gomez, P.A. Michaud, M.A. Rodrigo, Ch. Comninellis, Electrogeneration of hydroxyl radicals on boron-doped diamond electrodes, J. Electrochem. Soc. 150 (2003) D79-D83.

[15] V. Lam, G. Li, Ch. Song, J. Chen, C. Fairbridge, A review of electrochemical desulfurization technologies for fossil fuels, Fuel Process. Technol. 98 (2012) 30-38.

519 [16] W. Wang, S. Wang, Y. Wang, H. Liu, Z. Wang, A new approach to deep
520 desulfurization of gasoline by electrochemically catalytic oxidation and extraction,
521 Fuel Process. Technol. 88 (2007) 1002-1008.
522 [17] W. Wang, S. Wang, H. Liu, Z. Wang, Desulfurization of gasoline by a new method of
523 electrochemical catalytic oxidation, Fuel 86 (2007) 2747-2753.
524 [18] X.D. Tang, T. Hu, J.J. Li, F. Wang, D.Y. Qing, Deep desulfurization of condensate
525 gasoline by electrochemical oxidation and solvent extraction, RSC Adv. 5 (2015)
526 53455-53461.
527 [19] Z. Alipoor, A. Behrouzifar, S. Rowshanzamir, M. Bazmi, Electrooxidative
528 desulfurization of a thiophene-containing model fuel using a square wave
529 potentiometry technique, Energy Fuels 29 (2015) 3292-3301.
530 [20] X. Du, Y. Yang, C. Yi, Y. Chen, C. Cai, Z. Zhang, Preparation of AAO-CeO_2
531 nanotubes and their application in electrochemical oxidation desulfurization of diesel,
532 Nanotechnology 28 (2017) 065708.
533 [21] D. Julião, A.C. Gomes, M. Pillinger, R. Valença, J.C. Ribeiro, I.S. Gonçalves, S.S.
534 Balula, Desulfurization of liquid fuels by extraction and sulfoxidation using H_2O_2 and
535 [$CpMo(CO)_3R$] as catalysts, Appl. Catal. B: Environ. 230 (2018) 177-183.
536 [22] D. Liu, M. Li, R.L. Al-Otaibi, L. Song, W. Li, Q. Li, H.O. Almigrin, Z. Yan, Study on
537 the desulfurization of high-sulfur crude oil by the electrochemical method, Energy
538 Fuels 29 (2015) 6928-6934.
539 [23] X.D. Tang, T. Hu, J.J. Li, F. Wang, D.Y. Qing, Desulfurization of kerosene by the
540 electrochemical oxidation and extraction process, Energy Fuels 29 (2015) 2097-2103.
541 [24] C. Shu, T. Sun, J. Jia, Z. Lou, A novel desulfurization process of gasoline via sodium
542 metaborate electroreduction with pulse voltage using a boron-doped diamond thin film
543 electrode, Fuel 113 (2013) 187-195.

[25] M. Panizza, G. Cerisola, Influence of anode material on the electrochemical oxidation of 2-naphthol. Part 1. Cyclic voltammetry and potential step experiments, Electrochim. Acta 48 (2003) 3491-3497.

[26] A. Jailson-Cabral da Silva, E. Vieira dos Santos, C.C. de Oliveira-Morais, C.A. Martínez-Huitle, S. Souza Leal Castro, Electrochemical treatment of fresh, brine and saline produced water generated by petrochemical industry using Ti/IrO_2-Ta_2O_5 and BDD in flow reactor, Chem. Eng. J. 233 (2013) 47-55.

[27] A.R.F. Pipi, I. Sirés, A.R. De Andrade, E. Brillas, Application of electrochemical advanced oxidation processes to the mineralization of the herbicide diuron, Chemosphere 109 (2014) 49-55.

[28] S. Lanzalaco, I. Sirés, A. Galia, M.A. Sabatino, C. Dispenza, O. Scialdone, Facile crosslinking of poly(vinylpyrrolidone) by electro-oxidation with IrO_2-based anode under potentiostatic conditions, J. Appl. Electrochem. 48 (2018) 1343-1352.

[29] I. Sirés, E. Brillas, M.A. Oturan, M.A. Rodrigo, M. Panizza, Electrochemical advanced oxidation processes: Today and tomorrow. A review, Environ. Sci. Pollut. Res. 21 (2014) 8336-8367.

[30] M. Panizza, E. Brillas, Ch. Comninellis, Application of boron-doped diamond electrodes for wastewater treatment, J. Environ. Eng. Manage. 18 (2008) 139-153.

[31] H. Zanin, R.F. Teófilo, A.C. Peterlevitz, U. Oliveira, J.C. de Paiva, H.J. Ceragioli, E.L. Reis, V. Baranauskas, Diamond cylindrical anodes for electrochemical treatment of persistent compounds in aqueous solution, J. Appl. Electrochem. 43 (2013) 323-330.

[32] S. Mitroka, S. Zimmeck, D. Troya, J.M. Tanko, How solvent modulates hydroxyl radical reactivity in hydrogen atom abstractions, J. Am. Chem. Soc. 132 (2010) 2907-2913.

568 [33] E. Méndez-Albores, M. González-Fuentes, M.M. Dávila-Jiménez, F.J. González, Role
569 of water in the formation of sulfoxide and sulfone derivatives during the
570 electrochemical oxidation of dibenzothiophene in acetonitrile, J. Electroanal. Chem.
571 751 (2015) 7-14.
572 [34] G. Bontempelli, F. Magno, G.A. Mazzocchin, Cyclic and A.C. voltammetric study of
573 dibenzothiophene in acetonitrile medium, J. Electroanal. Chem. Interfacial
574 Electrochem. 43 (1973) 377-385.
575 [35] D.S. Houghton, A.A. Humffray, Anodic oxidation of diaryl sulphides-I. Diphenyl
576 sulphide in sulphate and perchlorate media, Electrochim. Acta 17 (1972) 1421-1433.
577 [36] P.T. Cottrell, C.K. Mann, Electrochemical oxidation of aliphatic sulfides under
578 nonaqueous conditions, J. Electrochem. Soc. 116 (1969) 1499-1503.
579 [37] J.L. Rivera, P. Navarro-Santos, L. Hernández-González, R. Guerra-González,
580 Reactivity of alkyldibenzothiophenes using theoretical descriptors, J. Chem. 2014
581 (2014) 1-8.
582 [38] Y. He, W. Huang, R. Chen, W. Zhang, H. Lin, Improved electrochemical performance
583 of boron-doped diamond electrode depending on the structure of titanium substrate, J.
584 Electroanal. Chem. 758 (2015) 170-177.
585 [39] J.N. Soderberg, A.C. Co, A.H.C. Sirk, V.I. Birss, Impact of porous electrode properties
586 on the electrochemical transfer coefficient, J. Phys. Chem. B 110 (2006) 10401-10410.
587 [40] J. Iniesta, P.A. Michaud, M. Panizza, G. Cerisola, A. Aldaz, Ch. Comninellis,
588 Electrochemical oxidation of phenol at boron-doped diamond electrode, Electrochim.
589 Acta 46 (2001) 3573-3578.
590 [41] J.F. Zhi, H.B. Wang, T. Nakashima, T.N. Rao, A. Fujishima, Electrochemical
591 incineration of organic pollutants on boron-doped diamond electrode. Evidence for
592 direct electrochemical oxidation pathway, J. Phys. Chem. B 107 (2003) 13389-13395.

[42] E.N. Al-Shafei, Process for in-situ electrochemical oxidative generation and conversion of organosulfur compounds, U.S. Patent, No. US 2013/0053578 A1, 2013.

[43] T. Kashiwada, T. Watanabe, Y. Ootani, Y. Tateyama, Y. Einaga, A study on electrolytic of boron-doped diamond electrodes when decomposing organic compounds, ACS Appl. Mater. Interfaces 8 (2016) 28299-28305.

[44] G.A. Orjuela, R. Rincón, J.J. Olaya, Corrosion resistance of niobium carbide coatings produced on AISI 1045 steel via thermo-reactive diffusion deposition, Surf. Coat. Tech. 259 (2014) 667-675.

Figure captions

Fig. 1. Chemical structure of dibenzothiophene (DBT), 4-methyldibenzothiophene (4-MDBT), and 4,6-dimethyldibenzothiophene (4,6-DMDBT).

Fig. 2. Linear sweep voltammograms obtained on a 20 cm^2 BDD electrode immersed in 80 mL of 67 mg L^{-1} DBT in different electrolytes: (a) Acetonitrile (87.5%)-water (12.5%, 0.01 M $NaNO_3$), (b) acetonitrile (12.5%)–water (87.5%, 0.01 M $NaNO_3$) and (c) water (100%, 0.01 M $NaNO_3$). Scan rate 10 mV s^{-1}.

Fig. 3. a, linear polarization curves on a BDD electrode recorded in acetonitrile (87.5%)-water (12.5%, 0.01 M $NaNO_3$), (------) in the absence of dibenzothiophene or in the presence of (a) 67 mg L^{-1} DBT, (b) 86 mg L^{-1} 4-MDBT and (c) 86 mg L^{-1} 4,6-DMDBT. b, after subtracting the background current from the (a') 67 mg L^{-1} DBT curve, (b') 86 mg L^{-1} 4-MDBT curve and (c') 86 mg L^{-1} 4,6-DMDBT. Scan rate 10 mV s^{-1}.

Fig. 4. a, consecutive cyclic voltammograms (cycles 1–5) on a BDD anode in acetonitrile (87.5%)-water (12.5%, 0.01 M $NaNO_3$), (------) in the absence of dibenzothiophene or in the presence of (a) 67 mg L^{-1} DBT, (b) 86 mg L^{-1} 4-MDBT and (c) 86 mg L^{-1} 4,6-DMDBT. b, (a) consecutive cycles (1–5) for 200 mg L^{-1} DBT and (b) consecutive cycles (1-44) for 200 mg L^{-1} 4,6-DMDBT under the same conditions. Scan rate 10 mV s^{-1}.

Fig. 5. Cyclic voltammograms recorded using a BDD anode in acetonitrile (87.5%)-water (12.5%, 0.01 M $NaNO_3$). (------) in the absence of dibenzothiophene. In a, (a) 30 mg L^{-1}, (b) 67 mg L^{-1} and (c) 100 mg L^{-1} of DBT. In b, (a') 30 mg L^{-1} (b') 100 mg L^{-1} and (c') 150 mg L^{-1} of 4,6-DMDBT. The inset panels show the corresponding Tafel analysis. Scan rate 10 mV s^{-1}.

623 **Fig. 6.** Linear sweep voltammograms obtained after subtracting the background current in
624 acetonitrile (87.5%)-water (12.5%, 0.01 M $NaNO_3$). In a, (a) 30 mg L^{-1}, (b), 67 mg L^{-1} and
625 (c) 100 mg L^{-1} of DBT. In b, (a') 30 mg L^{-1}, (b'), 100 mg L^{-1} and (c') 150 mg L^{-1} of 4,6-
626 DMDBT. The upper insets show *I* vs. concentration at 1774 mV in fig. a or 1884 mV in fig.
627 b. The lower insets show *E* vs. concentration at 0.525 (curve 1) or 0.750 mA (curve 2) in fig.
628 and b, respectively. Scan rate 10 mV s^{-1}.

629 **Fig. 7.** Potentiostatic *I–t* curves in quiescent solutions recorded (---) in the absence of
630 dibenzothiophene or in the presence of different 4,6-DMDBT concentrations: In a, (a) 30 mg
631 L^{-1}, (b) 86 mg L^{-1} and (c) 200 mg L^{-1} at E_{an} = 1.15 V; in b, (a) 30 mg L^{-1}, (b) 100 mg L^{-1}
632 and (c) 150 mg L^{-1} at E_{an} = 1.50 V; and in c, (a) 30 mg L^{-1}, (b) 86 mg L^{-1}, (c) 100 mg L^{-1}
633 and (d) 200 mg L^{-1} at E_{an} = 2.00 V. In the insets, the slope of the linear correlations was: a,
634 0.217 μA mg L^{-1}; b, 2.89 μA mg L^{-1}; and c, 5.84 μA mg L^{-1}.

635 **Fig. 8.** Chronoamperometric response of the BDD anode during the step-by-step injection of
636 a, water or b, 4,6-DMDBT into the reaction system. The anodic potential was 1.75 V. The
637 arrows indicate the injection into the reaction system of water (**ϙ**) or 4,6-DMDBT (↓). The
638 insets show *I* vs. the corresponding concentration.

639 **Fig. 9.** Scheme for the electrochemical oxidation of 4,6-DMDBT to yield the corresponding
640 sulfoxide and sulfone at 1.50 and 2.00 V in acetonitrile (87.5%)-water (12.5%, 0.01 M
641 $NaNO_3$).

642 **Fig. 10.** Scheme for the electrochemical oxidation of a mixture of DBT + 4-MDBT + 4,6-
643 DMDBT to yield their corresponding sulfoxides and sulfones at 1.50 and 2.00 V in
644 acetonitrile (87.5%)-water (12.5%, 0.01 M $NaNO_3$).

Fig. 11. Oxidation reactions of the dibenzothiophene compounds with hydrogen peroxide generated *in situ* by water electrolysis.

Fig. 12. Scheme of the direct electrochemical oxidation of dibenzothiophene compounds on a BDD anode in acetonitrile (87.5%)-water (12.5%, 0.01 M $NaNO_3$).

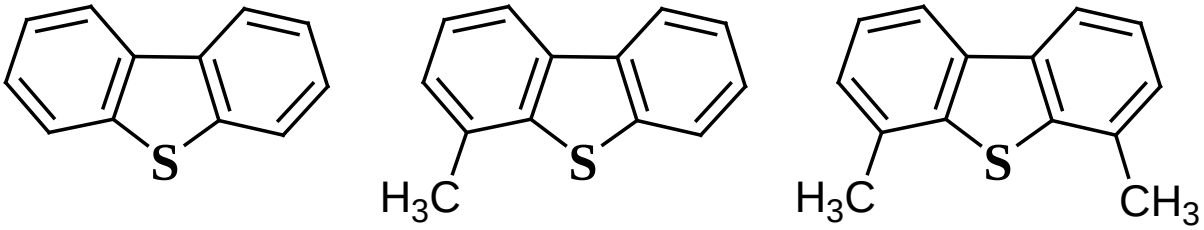

DBT 4-MDBT 4,6-DMDBT

Fig. 1

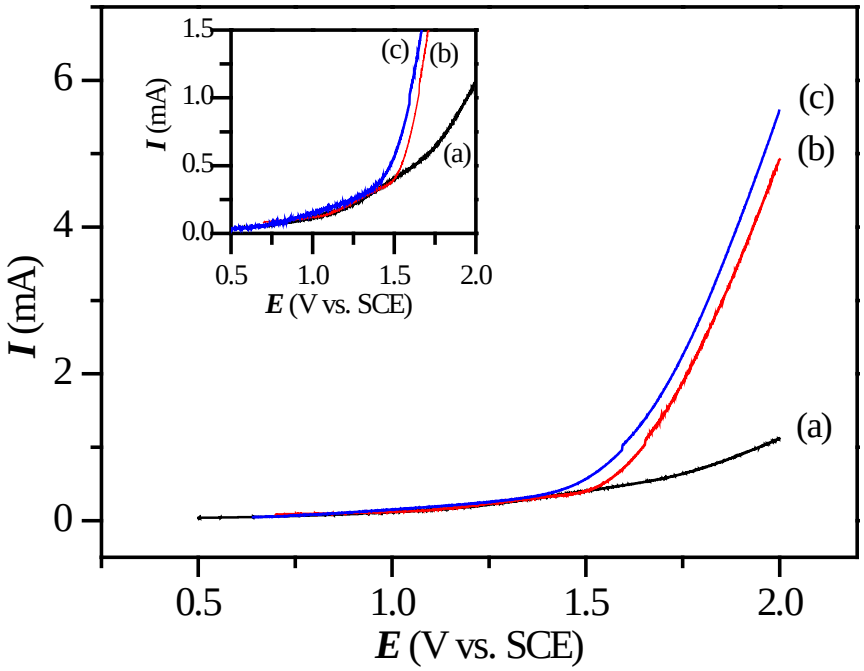

Fig. 2

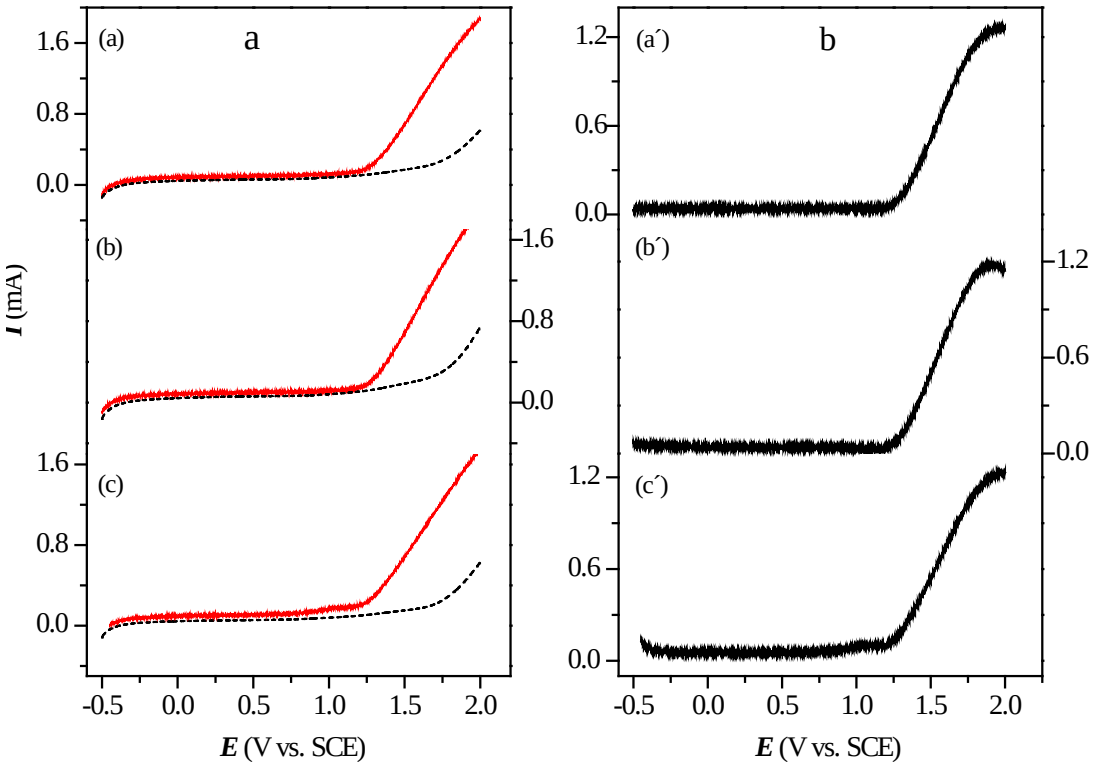

Fig. 3

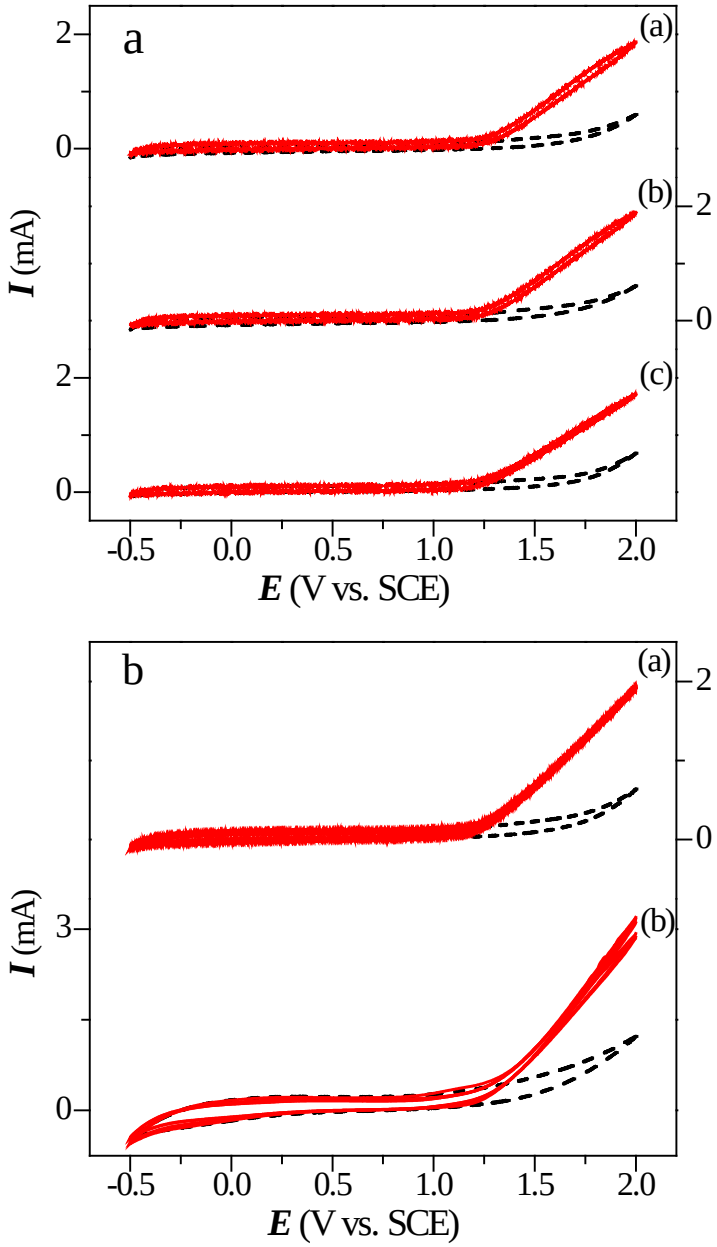
a
(a)
(b)
(c)
2
0
2
0
2
0
I (mA)
-0.5
0.0
0.5
1.0
1.5
2.0
E (V vs. SCE)
b
(a)
(b)
2
0
3
0
I (mA)
-0.5
0.0
0.5
1.0
1.5
2.0
E (V vs. SCE)

Fig. 4

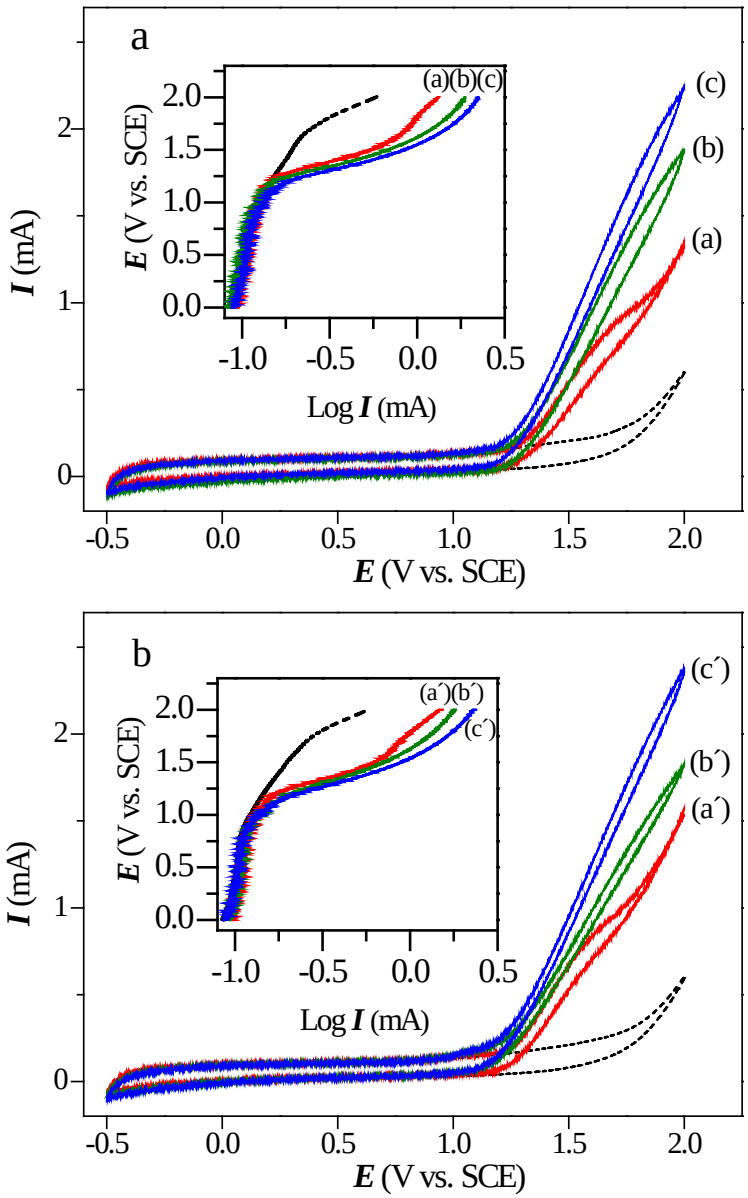
a
(a)(b)(c)
(c)
(b)
(a)
E (V vs. SCE)
Log I (mA)
I (mA)
E (V vs. SCE)
b
(a´)(b´)
(c´)
(c´)
(b´)
(a´)
E (V vs. SCE)
Log I (mA)
I (mA)
E (V vs. SCE)

Fig. 5

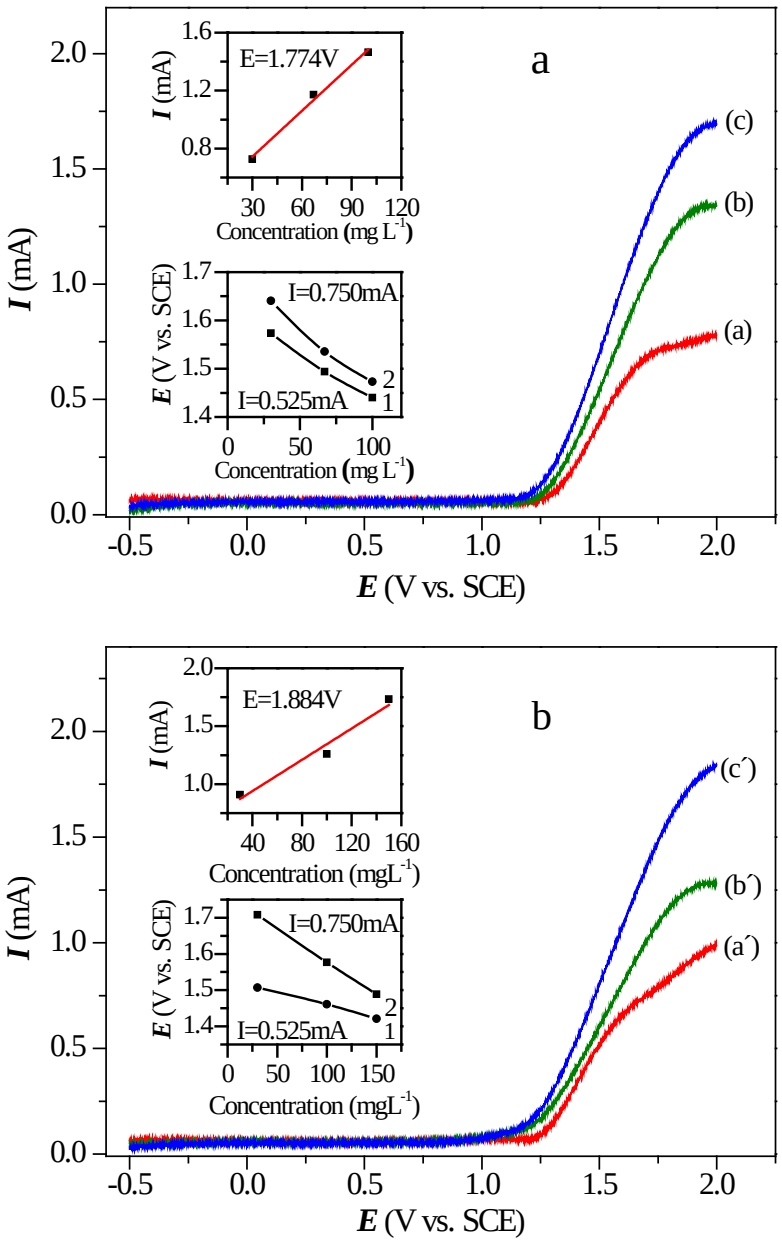
a
E=1.774V
I (mA)
Concentration (mg L-1)
E (V vs. SCE)
I=0.750mA
I=0.525mA
(a)
(b)
(c)
E (V vs. SCE)
b
E=1.884V
Concentration (mgL-1)
(a´)
(b´)
(c´)

Fig. 6

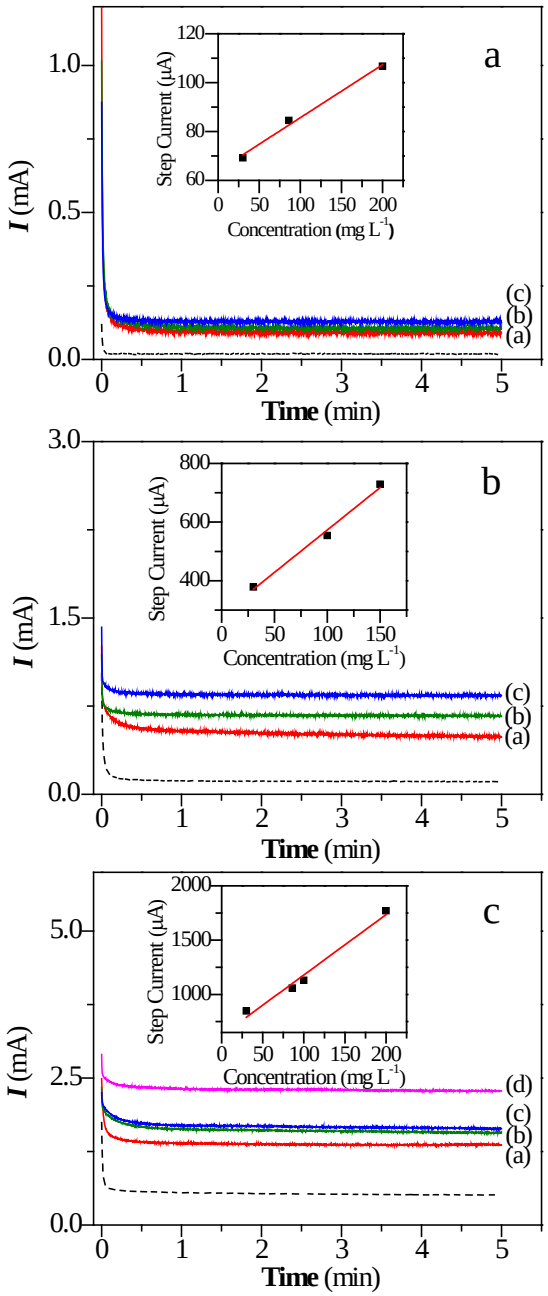

Fig. 7

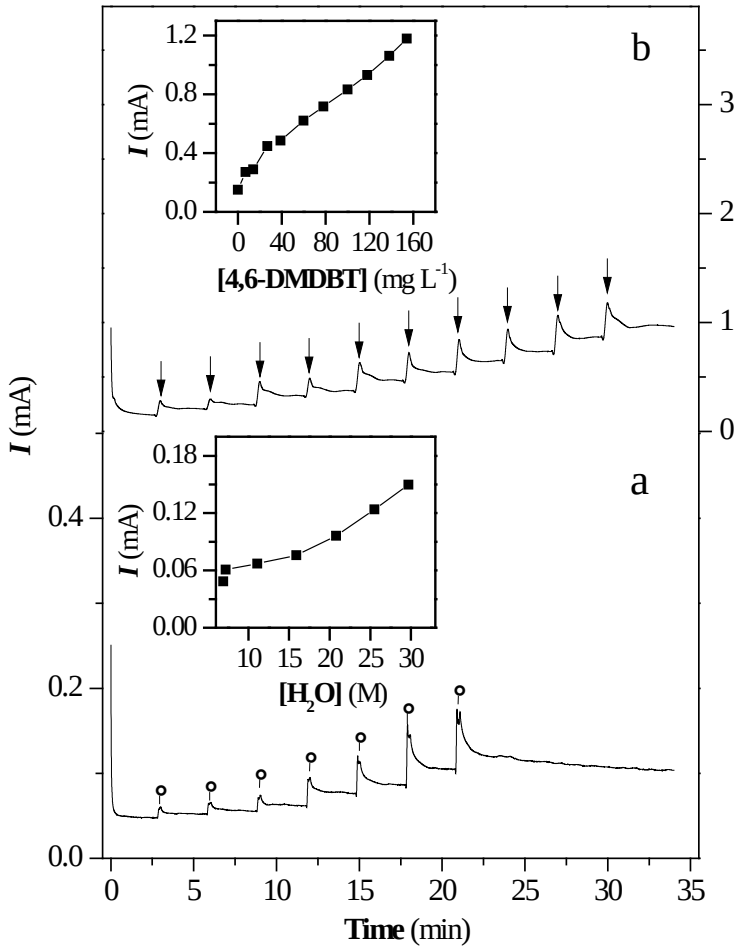

Fig. 8

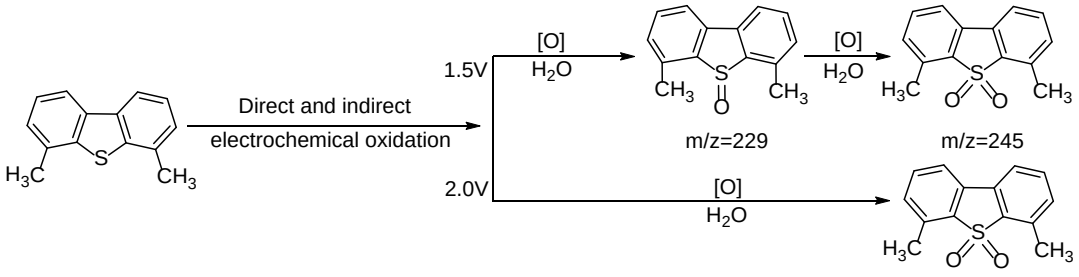
Direct and indirect
electrochemical oxidation
1.5V
2.0V
[O]
H2O
[O]
H2O
[O]
H2O
m/z=229
m/z=245
[O] - Oxidazing species type: •OH, HO2•, O3, O2•−, H2O2

Fig. 9

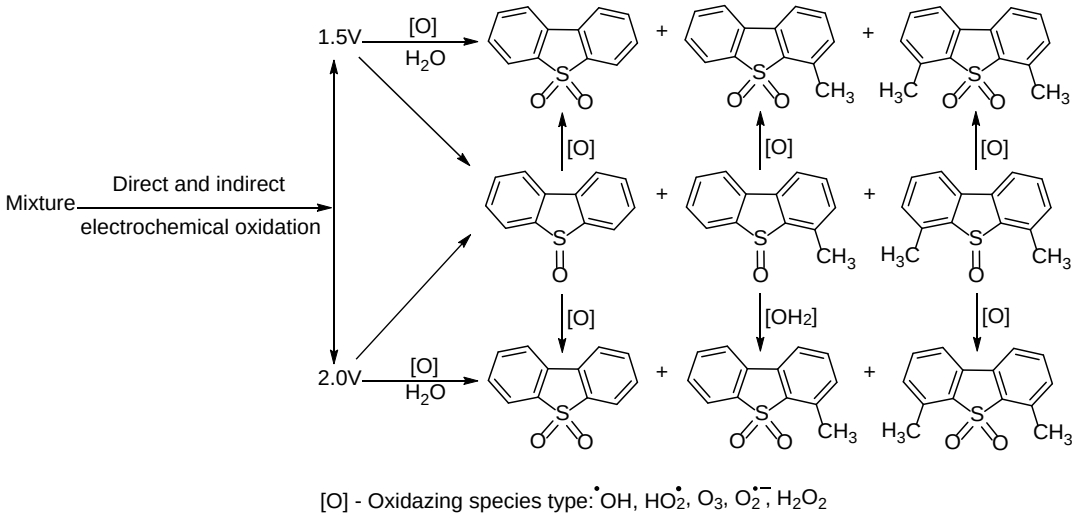
Mixture
Direct and indirect
electrochemical oxidation
1.5V
2.0V
[O]
H_2O
[O]
[O]
[O]
[O]
[OH_2]
[O]
[O] - Oxidazing species type: $^{\bullet}OH$, $HO_2^{\bullet}$, O_3, $O_2^{\bullet-}$, H_2O_2

Fig. 10

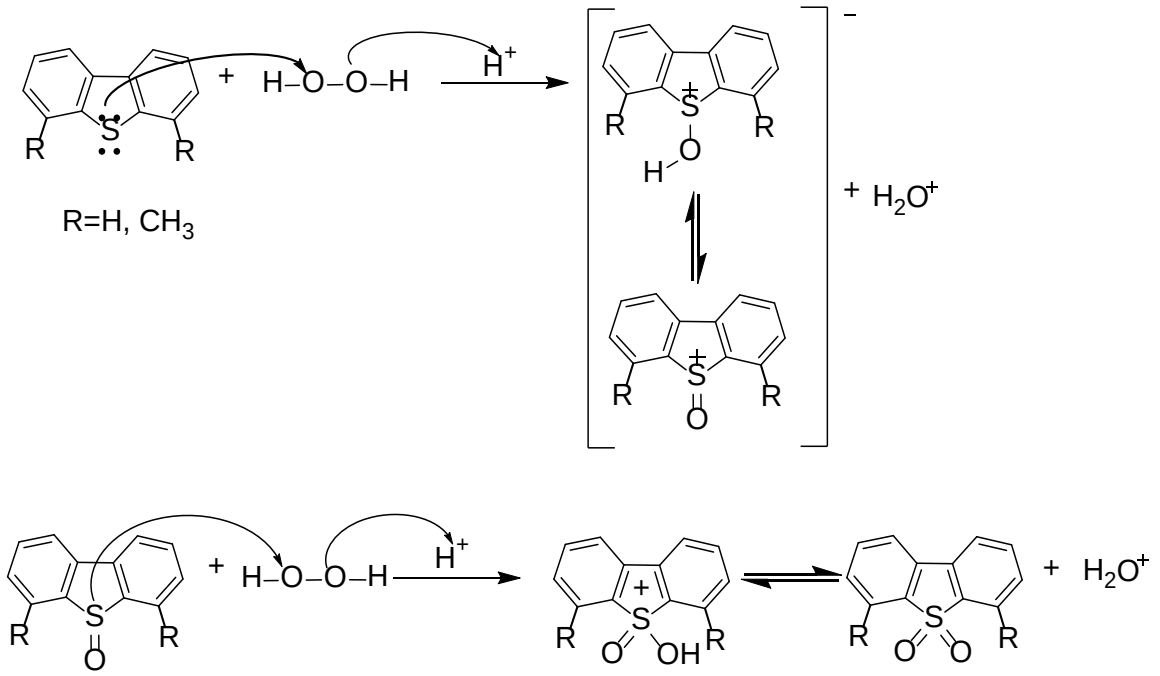

Fig. 11

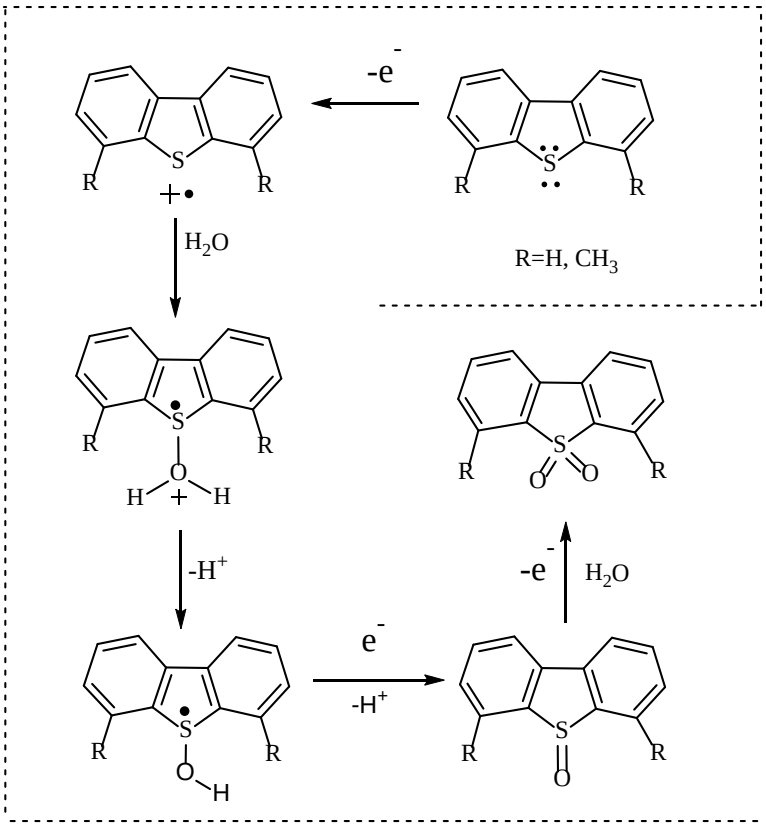

Fig. 12